



PERGAMON

International Journal of Heat and Mass Transfer 45 (2002) 255–265

International Journal of
**HEAT and MASS
TRANSFER**

www.elsevier.com/locate/ijhmt

Experimental study of pressurized gas-fluidized bed heat transfer

Art Yew Looi, Qi-Ming Mao, Martin Rhodes *

Department of Chemical Engineering, Monash University, P.O. Box 36, Clayton, VIC 3800, Australia

Received 24 May 2000; received in revised form 23 April 2001

Abstract

This paper reports on an experimental study of the influence of operating pressure, in the range 150–1100 kPa, on wall-to-bed heat transfer coefficient in a bubbling fluidized bed. Both Geldart Group A and B solids were studied and the fluidizing gases were air and superheated steam. Fluidizing velocities were in the range 1–33 U_{mf} and wall temperatures in the range 125–275°C. Wall-to-bed heat transfer coefficients were found to increase steadily with increasing fluidizing gas velocity and not to pass through a maximum. Increase in operating pressure was found generally to result in an increase in wall-to-bed heat transfer coefficient, although the effect is probably non-linear. In the bubbling regime, the wall-to-bed heat transfer coefficient was found to change with vertical position in the bed. Wall-to-bed heat transfer coefficients decreased when the bed entered the slugging regime. © 2001 Elsevier Science Ltd. All rights reserved.

Keywords: Fluidized bed; Pressure; Wall-to-bed heat transfer coefficient

1. Introduction

For want of fundamental understanding of the mechanisms involved, fluidized bed design procedures make frequent use of empirical correlations to relate easily the measurable input parameters to require output variables. With this approach, the intermediate levels between the input parameters and the output are essentially regarded as a black box and the reliability of these correlations depend on the degree of knowledge of this black box. Consequently, as pointed out by Botterill et al. [9], most of the heat transfer correlations available show consistent trends but they rarely agree with good accuracy.

The heat transfer coefficient between a submerged surface and the bed is usually taken to be the summation of radiative, particle convective and gas convective

components. The radiative component is usually neglected in a low temperature (below 500°C) system.

Gas convective heat transfer becomes significant when the superficial gas velocity is high or the particle size is large. At present, the most widely used gas convective heat transfer model is the one suggested by Baskakov et al. [2] and later corrected by Baskakov and Filipovsky [3].

Mickley and Fairbanks [18] proposed a particle convective heat transfer model in which heat is transferred from a hot surface to packets of solids which come in contact with the surface. These heated solids then migrate into the bulk of the fluidized bed. On the other hand, Botterill and Williams [11] considered the particles in a fluidized bed as discrete entities. The model presented by Botterill and Williams [11] describes heat being transferred to the particles in direct contact with the heat transfer surface and the energy is then transferred to the subsequent layers of particles.

Most of the fluidized bed heat transfer experimental data available are obtained at atmospheric pressure. It is common that these data are used to predict the heat transfer behaviour at elevated pressure, based on the mechanistic assumptions described above.

* Corresponding author. Tel.: +613-9905-3445; fax: +613-9905-5686.

E-mail address: martin.rhodes@eng.monash.edu.au (M. Rhodes).

Nomenclature			
A	heat transfer area (m ²)	Q_{loss}	heat loss through insulation (W)
d_p	particle size (m)	Q_o	heat output rate from band-heater (W)
h	wall-to-bed heat transfer coefficient (W/m ² K)	Δt	data logging time interval (s)
h_{max}	maximum wall-to-bed heat transfer coefficient (W/m ² K)	T_{wall}	wall temperature (°C)
Q_{in}	wall-to-bed heat input rate (W)	T_{bed}	fluidized bed temperature (°C)
		T_{lower}	lower section fluidized bed temperature (°C)
		T_{upper}	upper section fluidized bed temperature (°C)
		U_{mf}	minimum fluidization velocity (m/s)
		U_o	superficial gas velocity (m/s)

According to Xavier et al. [22], the change in pressure predominantly affects the gas convective component. It was further suggested that this effect is due to the variation of density of the interstitial gas in the dense phase. This argument is consistent with the experimental work reported by Botterill et al. [10], which shows that the heat transfer coefficient is greater when the fluidized bed pressure is higher. These authors also found that the influence of pressure on heat transfer coefficient diminishes with the reduction of particle size.

Most of the existing heat transfer models have a common parameter h_{max} . Despite its importance, the numerical prediction of h_{max} remains rather unsuccessful. Historically, the h_{max} phenomenon was first mentioned in the studies of tube-to-bed heat transfer. This was then extended to other fluidized bed heat transfer analyses regardless of the geometry of the heat transfer surface.

The transport phenomena on a vertical surface in a fluidized bed are very unlikely to be the same as those on a horizontal submerged surface. It is easy to perceive how the increasing bubble activity around a tube varies the overall heat transfer coefficient. However, there is very little evidence to relate the gas velocity or the bubble characteristics to the heat transfer resistance on a vertical surface. The increase in heat transfer coefficient on the fluidized bed wall as the gas velocity is raised from the point of incipient fluidization is not disputed, and in fact supported by experimental data provided by Bock, Borodulya et al., Botterill and Denloye, Grewal and Gupta and Molerus and Mattmann [5–7,14,19]. However, what is not obvious is the occurrence of a characteristic h_{max} . Furthermore, the experimental results reported by Gunn and Hilal [15] demonstrate a lack of certainty in h_{max} and this raises doubt on the reliability or usefulness of correlations predicting h_{max} for wall-to-bed heat transfer.

In this paper, we report on a study of the influence of pressure on wall-to-bed heat transfer in a bubbling fluidized bed. The study arises from a larger project looking at pressurized steam-fluidized bed drying of lignite the fuel used in power generation in the Australian state of Victoria.

2. Experiments

A pilot scale pressurized steam-fluidized bed dryer was designed and constructed for the purpose of this work. The process scheme was designed such that either pressurized superheated steam or air can be used as fluidizing medium.

A schematic diagram of the fluidized bed vessel is presented as Fig. 1. The vessel was made of carbon steel ASTM A106 Grade B. The straight cylindrical section, where the fluidized solids were contained, was assembled with two Schedule 80 pipes of 150 mm nominal bore, with a total length of approximately 1600 mm. The freeboard zone had an expanded head configuration with an expanded diameter of 400 mm nominal bore. The distributor was of a pseudo-bubble caps type. The distributor plate was conically inclined at approximately 5° from the horizontal reference. The purpose of this configuration was to ease the flow of solids towards the solid discharge nozzle. 26 bubble caps with threaded stem were locked onto the plate in a triangular arrangement with 25 mm equal pitch. The dimensions of the bubble caps are shown in Fig. 2.

For a simpler geometrical analysis, the fluidized bed wall was designated to be the heat transfer surface. There were two similar heating sections, as shown in Fig. 1. Each section consisted of three electrical band-heaters; the flanking band-heaters functioned as guard heaters for the middle one, where the heat transfer data were obtained. The guard heaters maintained zero temperature gradient on the vessel wall along the axial direction.

The fluidized bed temperature was measured at two separate positions. Each of these measuring points was located on the same horizontal level as the mid-point of the middle band-heater of each wall heating section. In order to determine the radial heat loss through the insulation, a thermocouple was placed on the outer surface of each middle band-heater and another thermocouple positioned on the outer cladding of the insulation on each corresponding horizontal level. All the process parameters were continuously recorded and the data acquisition rate was set at two cycles per minute.

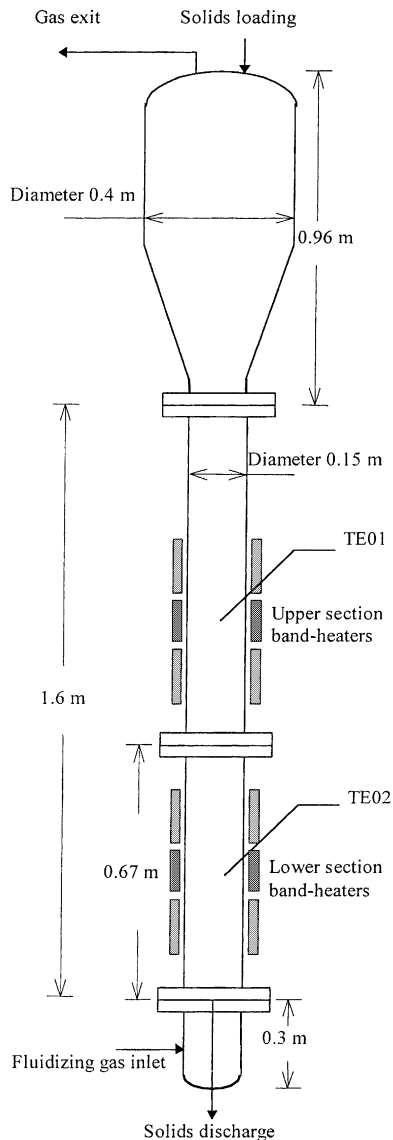


Fig. 1. Fluidized bed vessel.

2.1. Experimental procedure

Each of the experiments was carried out continuously for an extended period, during which a series of data was obtained at the pre-determined operating pressure, gas feed temperature and wall temperature, with the variation of the superficial fluidizing velocity. Each time the fluidizing velocity was changed, only the steady state data were considered for analyses. The steady-state conditions were maintained to facilitate the recording of at least 15 min of steady-data as the first set of results.

Some of the experiments were carried out with both heating sections being submerged by the fluidized bed while others were performed with just one active heating

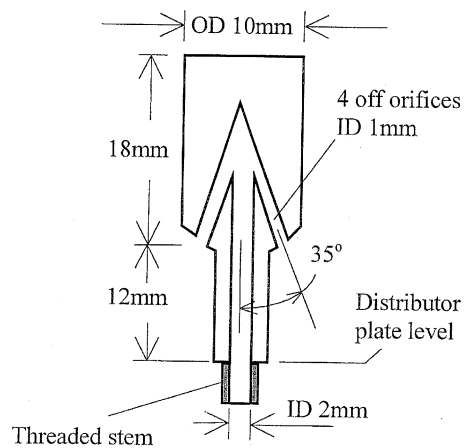


Fig. 2. Bubble-cap used as gas distributor.

sections covered by the fluidized solids. The operating conditions for all the experiments with both wall heating sections active are summarized and tabulated in Table 1 while those with single-section wall heating are presented in Table 2. Two types of solid particles, sand and porous alumina, were used. The surface-volume means particle sizes for sand and porous alumina are 201 and 105 μm , respectively. The particle densities for sand and alumina were 2660 and 1380 kg/m^3 , respectively. Under ambient conditions in air, the sand would be classified as Geldart Group B whilst the alumina would be Group A.

2.2. Data analysis

The radial rate of heat transfer into the fluidized bed is calculated from Eq. (1).

$$Q_{\text{in}} = \frac{\sum(Q_o \Delta t) - \sum(Q_{\text{loss}} \Delta t)}{\sum(\Delta t)}, \quad (1)$$

where Q_{in} is the net radial rate of heat transfer into the bed while Q_o is the instantaneous rate of heat output from the middle band-heater of each wall heating section at the end of each corresponding data logging time interval, Δt . Q_{loss} is the calculated heat loss based on the instantaneous temperature gradient in the insulation. The logging time interval was set at 30 s.

The wall-to-bed heat transfer coefficient is calculated based on the generalized convective heat transfer relationship as described by Eq. (2)

$$Q_{\text{in}} = hA(T_{\text{wall}} - T_{\text{bed}}). \quad (2)$$

The heat transfer area is the area on the inside wall of the section covered by each middle band-heater. T_{bed} and T_{wall} are the time-averaged values over the steady-state period. The heat transfer coefficients determined at the upper and lower bed heating sections are denoted as h_{upper} and h_{lower} , respectively.

Table 1
Operating conditions for heat transfer experiments with both wall heating sections covered by the fluidized bed

Series	Solids	Gas	T_{feed} (°C)	P (kPa)	T_{wall} (°C)
FAA1	Alumina	Air	125	150	210
FAA2	Alumina	Air	125	300	210
FAS1	Sand	Air	126	150	210
FAS2	Sand	Air	121	300	210.0
FAS3	Sand	Air	65	300	210
FAS4	Sand	Air	65	300	100
FSS1	Sand	Steam	121	150	155
FSS2	Sand	Steam	143	300	155
FSS3	Sand	Steam	125	150	210
FSS4	Sand	Steam	167	600	210
FSS5	Sand	Steam	193	1100	210

Table 2
Operating conditions for heat transfer experiments with only one wall heating section covered by the fluidized bed

Series	Solids	Gas	T_{feed} (°C)	P (kPa g)	T_{wall} (°C)
HAA1	Alumina	Air	100	150	210
HAA2	Alumina	Air	125	150	210
HAA3	Alumina	Air	87	300	210
HAA4	Alumina	Air	125	300	210
HAA5	Alumina	Air	180	300	210
HAA6	Alumina	Air	200	300	210
HAA7	Alumina	Air	65	300	100
HSA1	Alumina	Steam	180	150	210
HSA2	Alumina	Steam	177	600	210
HSA3	Alumina	Steam	178	600	275
HSA4	Alumina	Steam	188	1100	210
HSA5	Alumina	Steam	188	1100	275

2.3. Results

The experimental results show that the heat transfer behaviour is not entirely homogeneous throughout the fluidized bed. Figs. 3–5 illustrate the difference between h_{upper} and h_{lower} during each experiment. It is noted that h_{upper} is consistently higher than h_{lower} when porous alumina was used as the fluidized bed material, as shown in Fig. 3. This phenomenon appears in the fluidization of sand (Figs. 4 and 5) only at the lower superficial gas velocity range. There is a general trend that $(h_{\text{upper}} - h_{\text{lower}})$ diminishes as U_o is increased. In order to determine whether this variation of heat transfer behaviour is an effect of the distance from the distributor or that from the surface of the fluidized bed, the experimental results of FAA1 and HAA2 were compared. The experiments of FAA1 and HAA2 were carried out with both wall heating sections being active while those of HAA2 only had the lower wall heating section submerged by the fluidized bed. The comparison shown in Fig. 6 indicates that the heat transfer behaviour is changing with distance from the distributor.

Figs. 7–9 show the effect of operating pressure on wall-to-bed heat transfer coefficient over the range

600–1100 kPa and with different combinations of solids and gas.

Fig. 10 shows the influence of the wall temperature T_{wall} on wall-to-bed heat transfer coefficient in the air–alumina and air–sand systems. The results indicate that there is effectively no difference in the heat transfer coefficient when the air-fluidized bed wall temperature is raised from 100°C to 210°C. However, there appears to be a more significant effect of T_{wall} on the h when steam acts as the fluidizing medium as indicated in Fig. 11. It is also noted in Fig. 11 that the increase in the wall-to-bed heat transfer coefficient due to a higher wall temperature is more obvious when the bed is fluidized at a higher gas velocity.

3. Discussion

All the experimental results presented show that there is no characteristic h_{max} in the wall-to-bed heat transfer. The existence of h_{max} in horizontal tube-to-bed heat transfer is attributed to the bubble shrouding on the horizontal heat transfer surface. This is unlikely to occur on a vertical wall since the bubble patterns tend

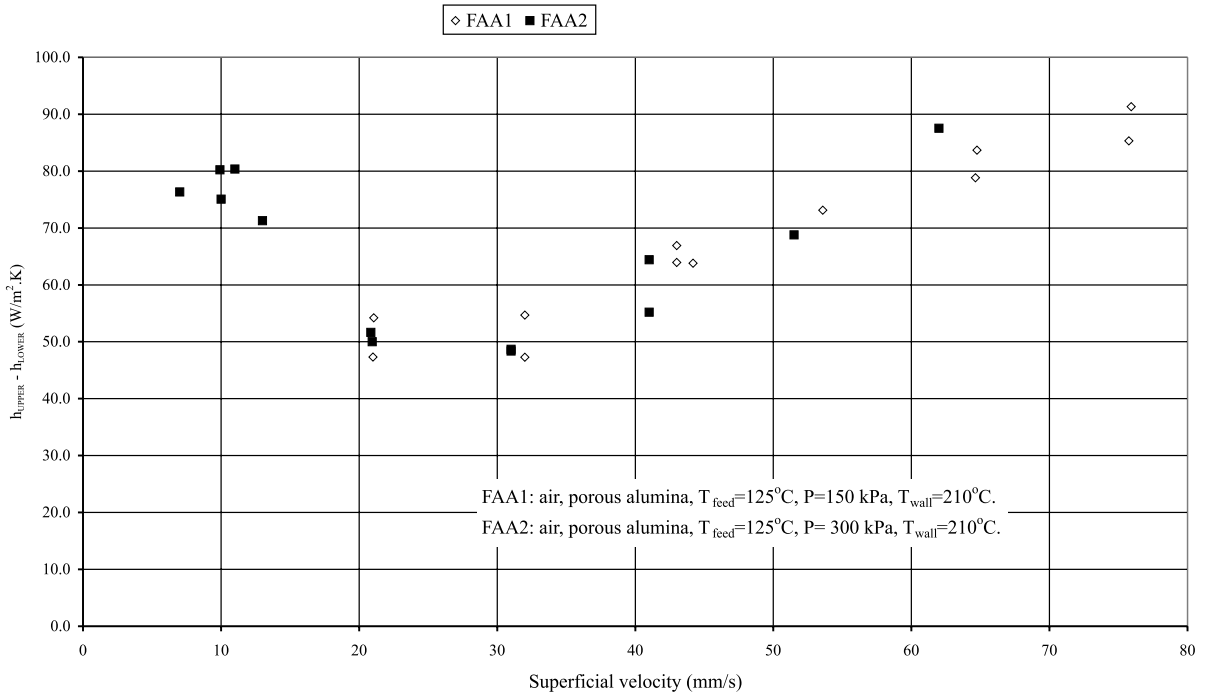


Fig. 3. $h_{upper} - h_{lower}$ for air-fluidized porous alumina experiments.

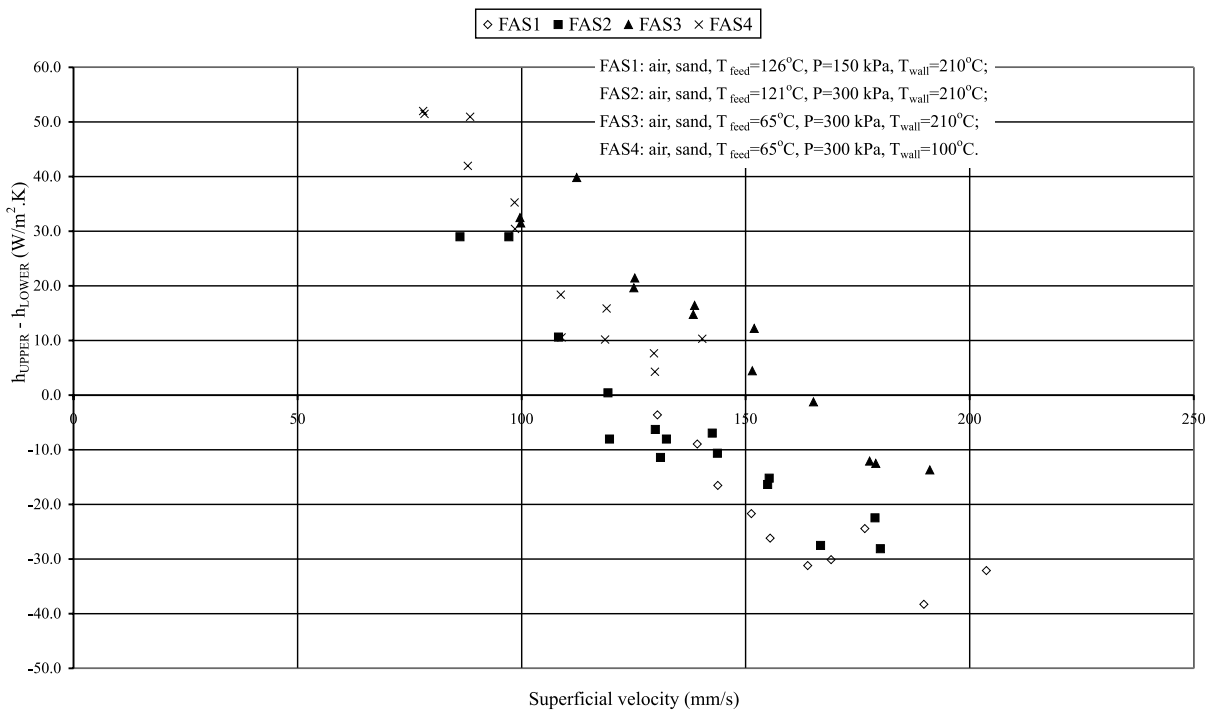


Fig. 4. $h_{upper} - h_{lower}$ for air-fluidized sand experiments.

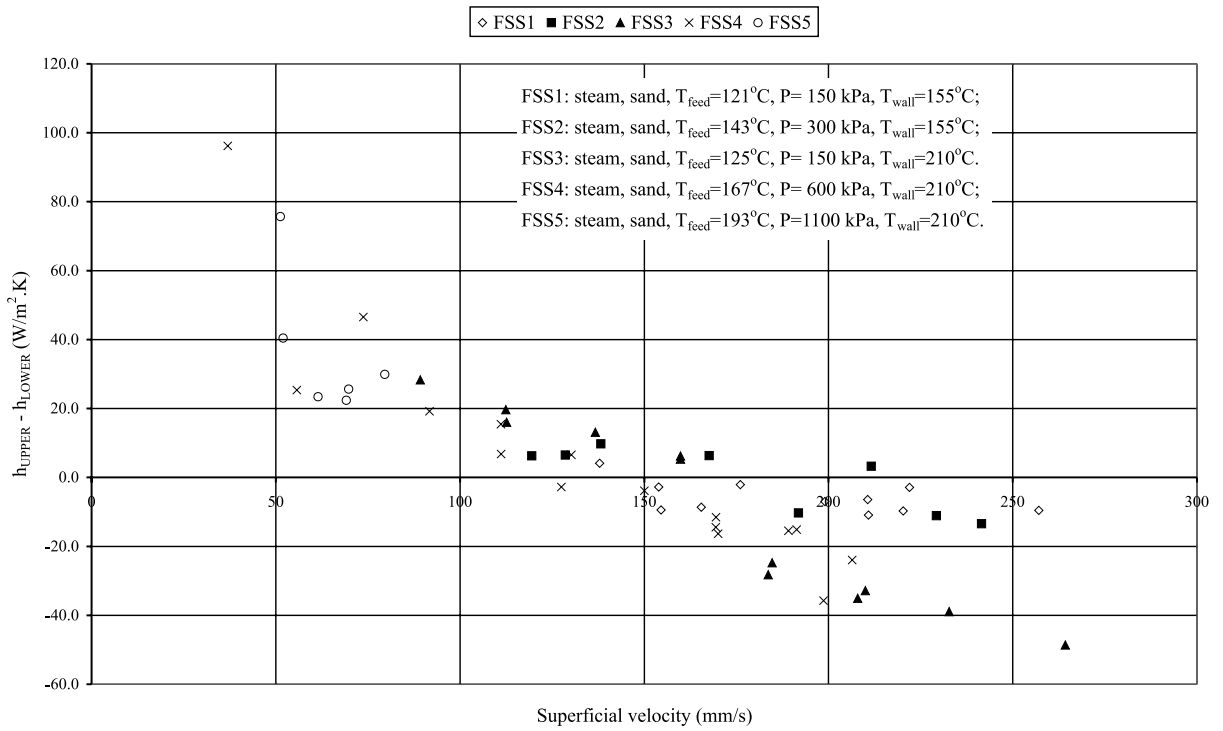


Fig. 5. $h_{\text{upper}} - h_{\text{lower}}$ for steam-fluidized sand experiments.

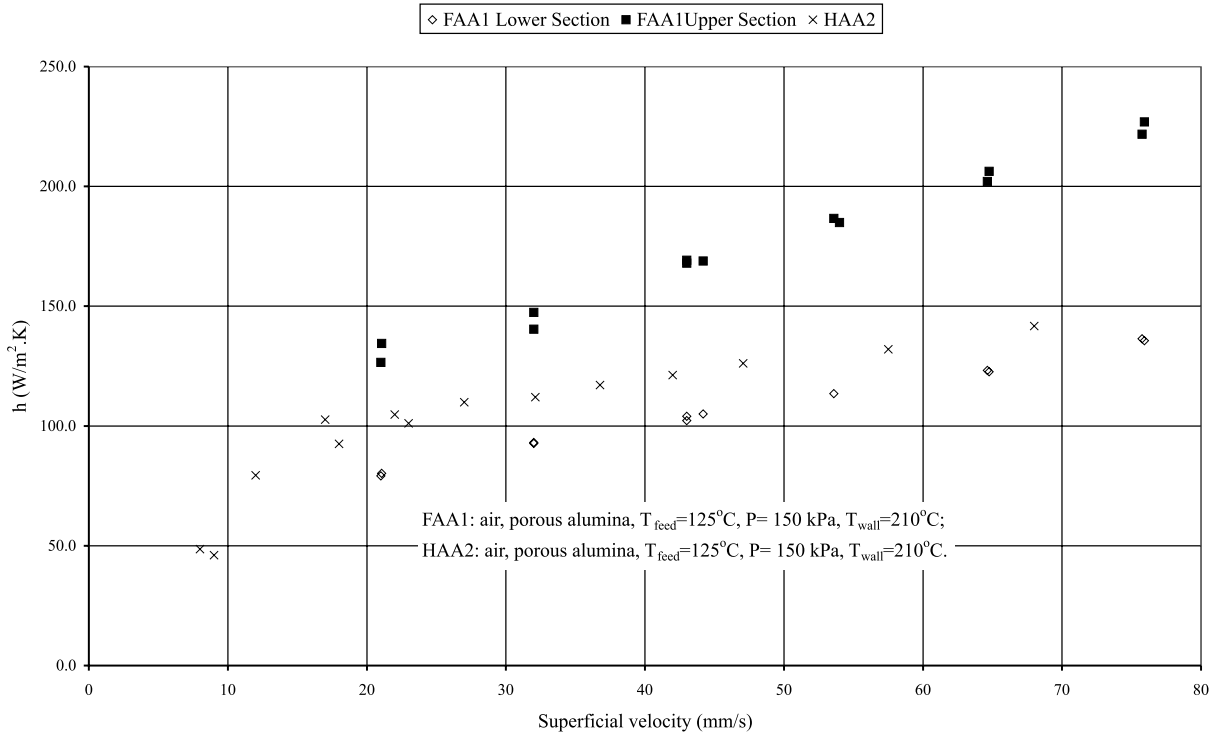


Fig. 6. Comparison of results from similar experiments of different bed depths.

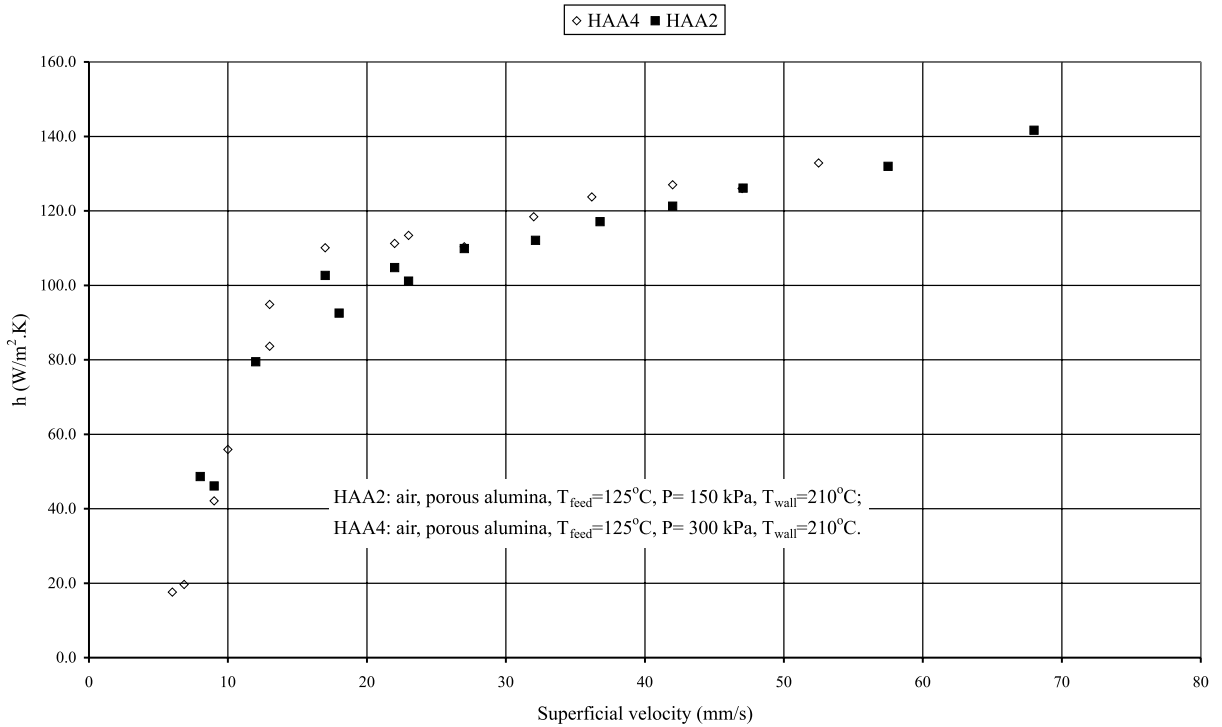


Fig. 7. Effect of pressure on wall-to-bed heat transfer coefficient in air-fluidized porous alumina experiments.

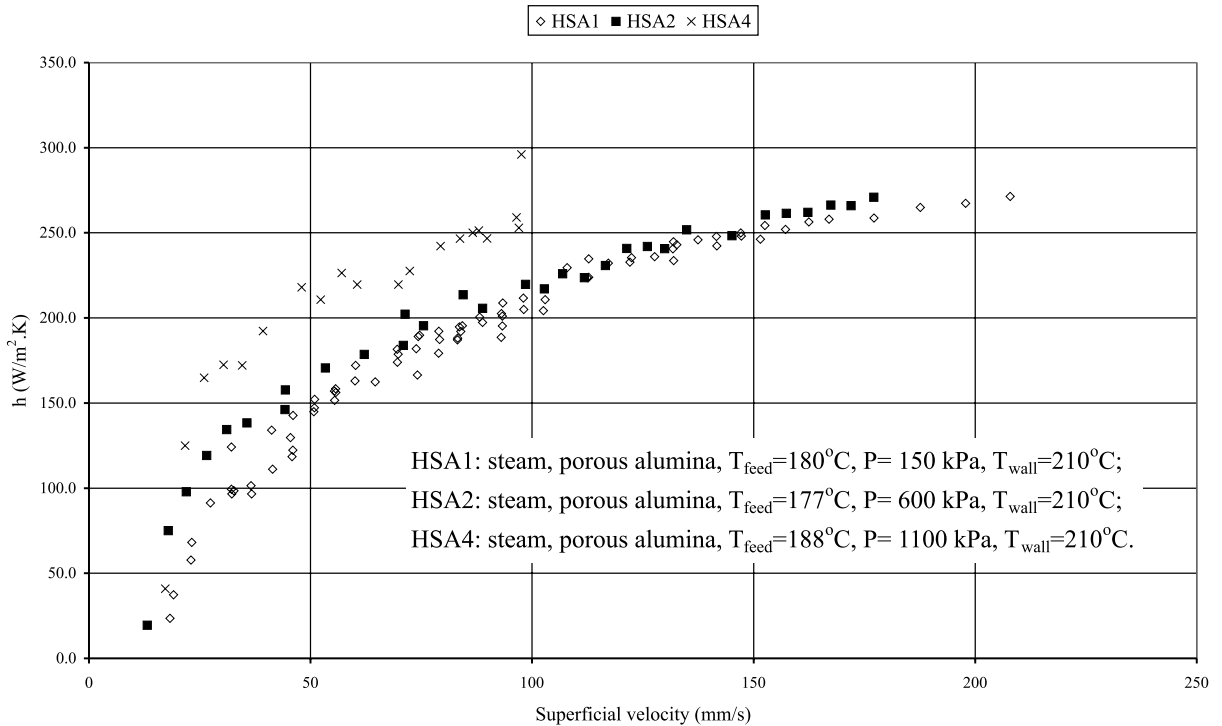


Fig. 8. Effect of pressure on wall-to-bed heat transfer coefficient in steam-fluidized porous alumina experiments.

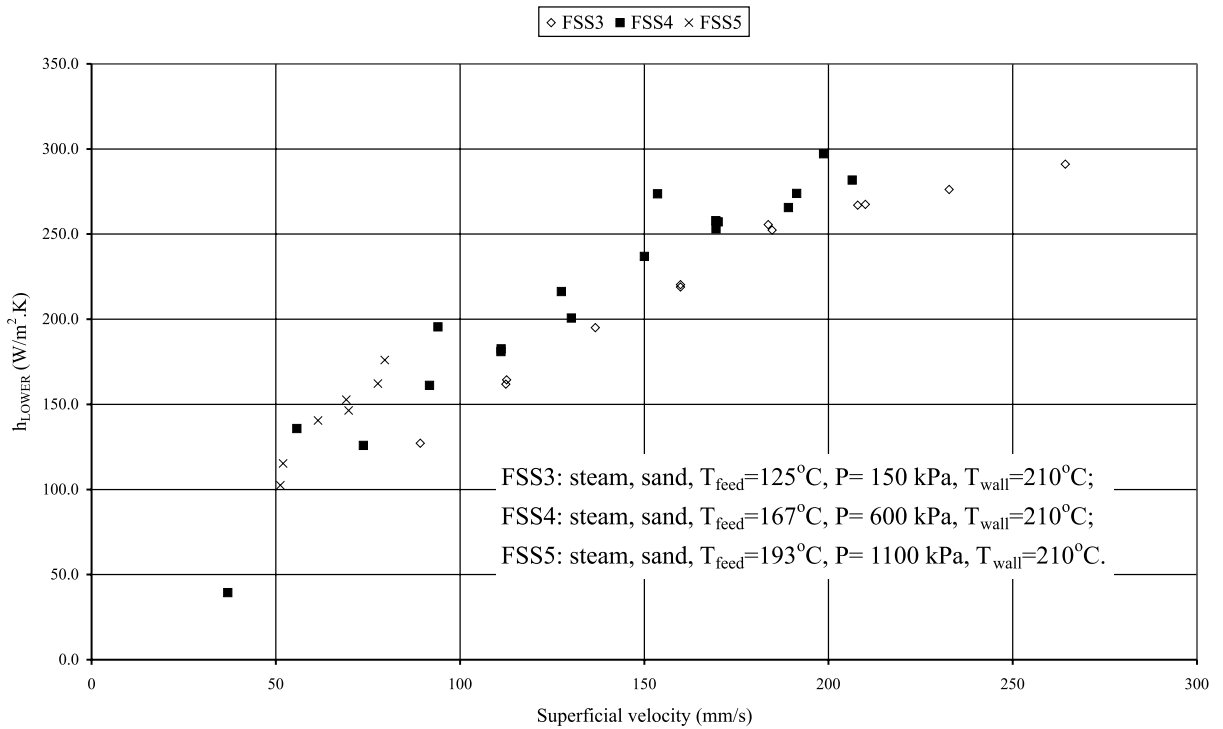


Fig. 9. Effect of pressure on wall-to-bed heat transfer coefficient in steam-fluidized porous sand experiments.

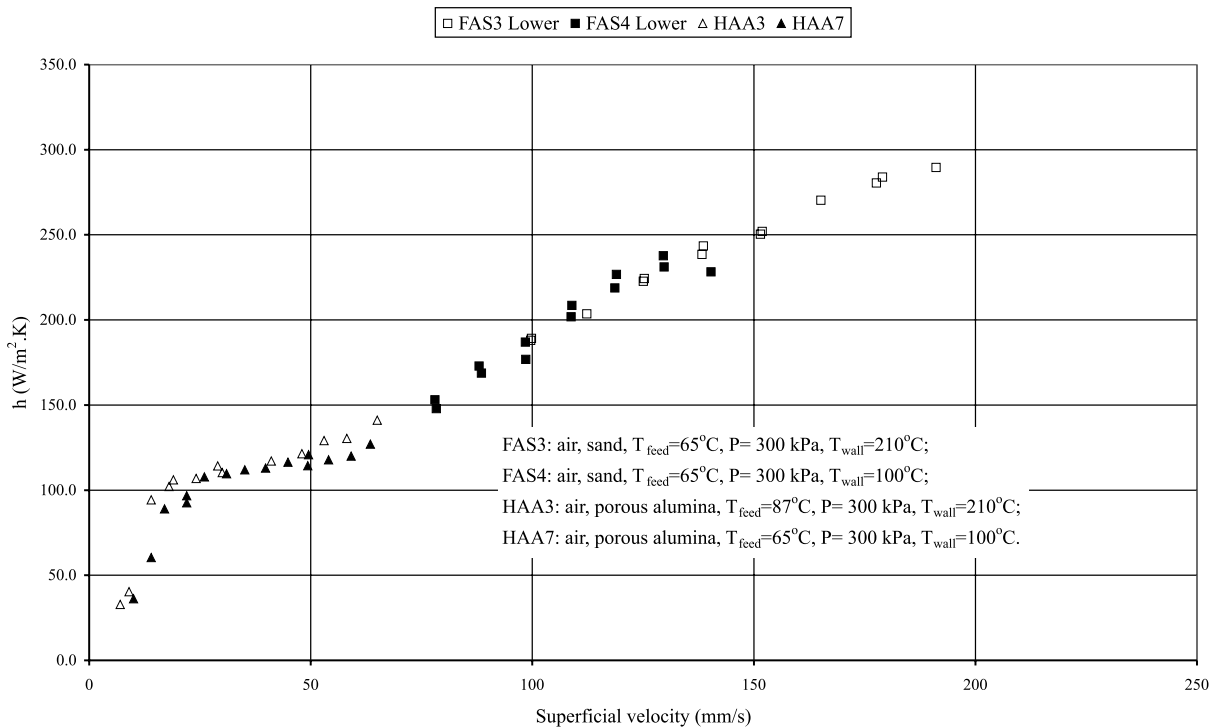


Fig. 10. Effect of wall temperature on wall-to-bed heat transfer coefficient in air-fluidized porous bed experiments.

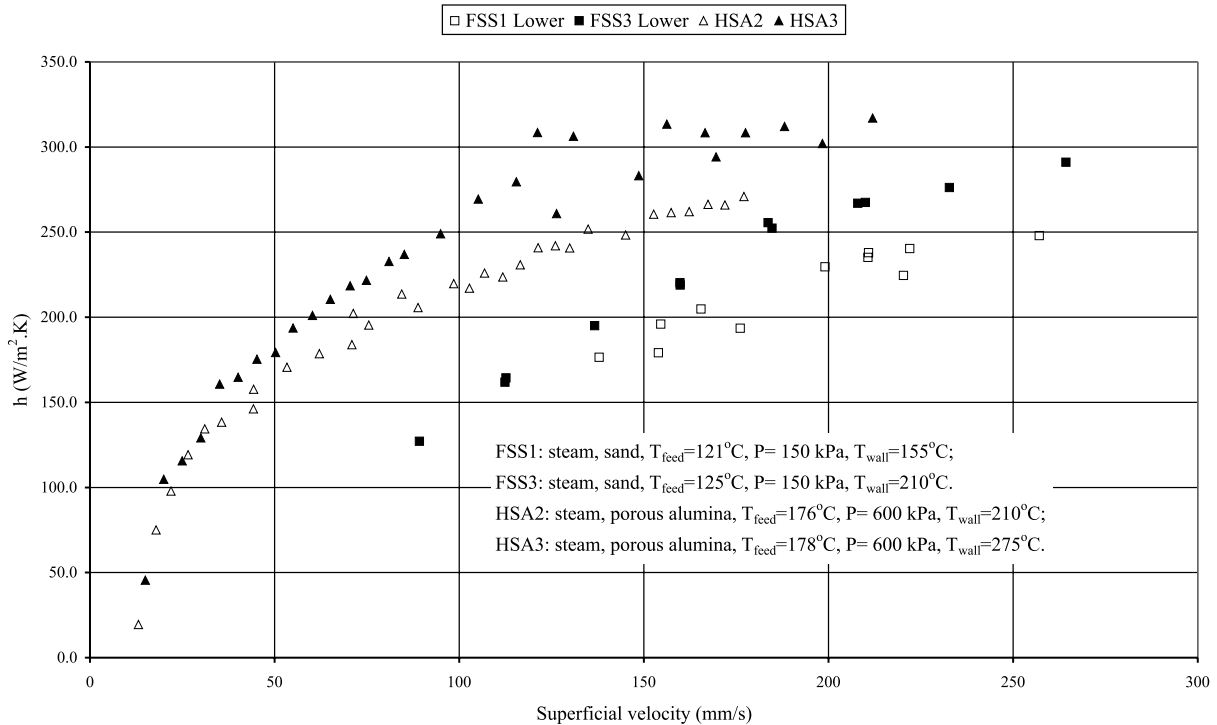


Fig. 11. Effect of wall temperature on wall-to-bed heat transfer coefficient in steam-fluidized porous bed experiments.

to drive the bubbles towards the centre of the fluidized bed.

Figs. 3–5 indicate that the wall-to-bed heat transfer coefficient in the gas-fluidized bed varies with axial position. Fig. 6 confirmed that the characteristic distance is that between the point of heat transfer measurement and the distributor. In Fig. 3, which shows the results of the air–alumina experiments, the heat transfer coefficient for the upper bed section h_{upper} is always greater than the heat transfer coefficient for the lower bed section, h_{lower} . In Figs. 4 and 5, which show the results of the air–sand and steam–sand experiments, h_{upper} is greater than h_{lower} at low velocities. However, the difference between h_{upper} and h_{lower} decreases as gas velocity is increased and in general h_{upper} is less than h_{lower} at high gas velocities. We will first examine the variation of heat transfer coefficient with vertical position in the bed and then look at why h_{upper} becomes smaller than h_{lower} at high gas velocities. Variation of wall-to-bed heat transfer coefficient with vertical position was also reported by Gunn and Hilal [15]; however, no explanation was offered by these authors. We suggest that this variation of heat transfer coefficient with vertical position in the bed may be due to improvement in solids circulation towards the upper section of the bed. In the case of sand fluidized by air for example, bubble size at a superficial gas velocity of 0.15 m/s (predicted by the correlation of Darton et al. [13]) increases from 5 cm in the lower bed section to 12 cm

in the upper section. The increase in bubble size is likely to result in increased solids circulation and increased rate of replacement of solids at the wall; this in turn may be the cause of the increased heat transfer coefficient with vertical position in the bed. Why then does h_{upper} become less than h_{lower} at high gas velocities? The possibility that this was caused by bed slugging was examined. The minimum slugging velocity U_{ms} for each set of conditions was estimated using the correlation of Stewart and Davidson [21]. U_{ms} was found to be of the order of 95 mm/s for experiments involving alumina and around 110 mm/s for the sand experiments. Only minor variations around these values result from changes in fluid properties. The critical bed depth, beyond which slugging would occur at superficial velocities greater than U_{ms} , was estimated using the correlation of Baeyens and Geldart [1] to be 0.43 m in all experiments. This suggests that slugging would occur only in the upper section, provided the velocity is high enough. Examining Figs. 3–5 again in this light we see that at gas velocities less than U_{ms} , h_{upper} is always greater than h_{lower} , as the gas velocity is increased the difference between h_{upper} and h_{lower} diminishes and at gas velocities greater than U_{ms} h_{lower} is greater than h_{upper} . We suggest that the reason for this is the decrease in the heat transfer coefficient in the upper section as the bed approaches and enters the slugging regime. This suggestion is supported by the results of Gunn and Hilal [15], who reported a rapid

drop in the heat transfer coefficient, with increasing gas velocity, due to the onset of slugging.

Although there is considerable scatter, the results shown in Figs. 7–9 confirm the observations of Botterill and Desai, Botterill et al. and Xavier et al. [8,10,22] that the heat transfer coefficient in the bubbling regime increases with increasing operating pressure. However, these results also suggest that as the bed moves into the slugging regime, the heat transfer coefficient is less affected by operating pressure. Also, the experimental results presented in Fig. 8 also show that the pressure effect on the heat transfer coefficient may not be linear. Several groups of researchers, such as Čärsky et al., Hoffmann and Yates, and Rowe et al. [12,16,20] have reported that the response of the fluidized bed behaviour to the variation of operating pressure is dependent on the pressure range. The change in operating pressure results in a change in the thermodynamic properties of the fluidizing gas. The variation of pressure also alters the transport properties of the gas. The most immediate outcome is the change in the bubble characteristics in the fluidized bed. This in turn influences the gas–solid interaction and the effectiveness of the wall-to-bed heat transfer. It is generally believed that increasing operating pressure reduces bubble size and gives rise to ‘smoother’ fluidization. However, quantitative information is hard to come by and just how a reduction in bubble size can give rise to an increase in heat transfer coefficient is unclear. These issues are the subject of a current investigation by the corresponding author.

Beeby and Potter [4] and Jensen [17], among others, have suggested that the enhancement of heat transfer between fluidized bed and a submerged surface when the operating pressure is raised is caused by the increase in the thermal conductivity of the fluidizing gas. In order to verify this assumption, experiments were conducted with T_{wall} being varied, which would directly alter the fluid properties on the heat transfer surface, while maintaining the other operating parameters constant.

The thermal conductivity of 300 kPa air at 100°C and 210°C is 0.032 and 0.039 W/m K, respectively. If the assumption that enhancement of heat transfer at higher pressure is due to the improved gas thermal conductivity is true, the measured heat transfer coefficient in HAA3 would have been greater than that in HAA7. Similarly, the measured heat transfer coefficient in FAS3 would have been greater than that in FAS4. However, Fig. 10 shows that there is effectively no difference in the wall-to-bed heat transfer coefficient between HAA3 and HAA7 or FAS3 and FAS4.

Fig. 11 illustrates that the variation of T_{wall} has a more significant effect on h in a steam-fluidized bed. The thermal conductivity of steam on the wall in FSS1 and FSS3 is 0.029 and 0.034 W/m K, respectively, while the thermal conductivity of steam on the wall in HSA2 and HSA3 is 0.036 and 0.042 W/m K, respectively. The ex-

perimental results show that at sufficiently high U_0 , the wall-to-bed heat transfer coefficient increases in the same proportion as the increase in the thermal conductivity of steam on the wall. This finding lends some support to the assumption that the enhancement of heat transfer coefficient when pressure is elevated is attributed to the improved gas thermal conductivity on the heat transfer surface. However, the results presented in Fig. 10 suggest that this may not be the controlling factor for all fluidizing media and that the broader issue of solids motion against the heat transfer surface must be taken into account.

4. Conclusion

Based on the results of this experimental study of the influence of operating pressure on the wall-to-bed heat transfer coefficient in a gas-fluidized bed, we conclude that:

- (i) This heat transfer coefficient generally increases with increasing pressure, although the relationship may not be linear.
- (ii) The conductivity of the gas adjacent to the heat transfer surface may have a controlling role under some conditions but not under others.
- (iii) The influence of bed dynamics on wall-to-bed heat transfer is important and may dominate in some circumstances.
- (iv) The wall-to-bed heat transfer coefficient increases steadily with fluidizing gas velocity and does not pass through a maximum.
- (v) In the bubbling bed the wall-to-bed heat transfer coefficient increases with increasing distance from the distributor.
- (vi) The wall-to-bed heat transfer coefficient decreases as the bed moves into the slugging regime as gas velocity is increased.

Further studies are required to evaluate the influence of operating pressure on bubble and solids motion in the bubbling bed with a view to understanding the mechanisms by which pressure influences wall-to-bed heat transfer coefficient.

References

- [1] J. Baeyens, D. Geldart, Chem. Eng. Sci. 29 (1974) 255.
- [2] A.P. Baskakov, B.V. Berg, O.K. Vitt, N.F. Filippovsky, V.A. Kirakosyan, J.M. Goldobin, V.K. MaskaeV, Heat transfer to objects immersed in fluidized beds, Powder Technol. 8 (1973) 273–282.
- [3] A.P. Baskakov, N.F. Filippovsky, A simple method of heat transfer calculations in fluidized bed furnaces, in: J.R. Grace, L.W. Shemilt, M.A. Bergougnou (Eds.), Fluidization VI, Proceedings of the International Conference on Fluidization, Banff, Alberta, Canada, May 7–12, 1989, Engineering Foundation, NY, 1989, pp. 695–700.

- [4] C. Beeby, O.E. Potter, Steam drying, in: R. Toie, A.S. Mujumdar (Eds.), *Drying '85*, 4th International Drying Symposium, Kyoto, Japan, July 9–12, 1984, Hemisphere, Washington, 1985.
- [5] H.J. Bock, Dimensioning of vertical heat transfer surface in gas/solid fluidized beds, *German Chem. Eng.* 4 (1981) 356–362.
- [6] V.A. Borodulya, V.G. Ganzha, A.I. Podberezsky, Heat transfer in a fluidized bed at high pressure, in: J.R. Grace, J.M. Matsen (Eds.), *Fluidization*, Proceedings of the 1980 International Fluidization Conference, Sponsored by the Engineering Foundation, Henniker, New Hampshire, August 3–8, 1980, Plenum Press, New York, 1980, pp. 201–206.
- [7] J.S.M. Botterill, A.O.O. Denloye, Gas convective heat transfer to packed and fluidized beds, *AIChE Symp. Ser.* 176 74 (1978) 194–202.
- [8] J.S.M. Botterill, M. Desai, Limiting factors in gas-fluidized bed heat transfer, *Powder Technol.* 6 (1972) 231–238.
- [9] J.S.M. Botterill, Y. Teoman, K.R. Yürengir, Factors affecting heat transfer between gas-fluidized beds and immersed surfaces, *Powder Technol.* 39 (1984) 177–189.
- [10] J.S.M. Botterill, Y. Teoman, K.R. Yürengir, The effect of operating temperature on velocity of minimum fluidization, bed voidage and general behaviour, *Powder Technol.* 31 (1982) 101–110.
- [11] J.S.M. Botterill, J.R. Williams, The mechanism of heat transfer to gas-fluidized beds, *Trans. Inst. Chem. Eng.* 41 (1963) 217–223.
- [12] M. Cársky, M. Hartman, B. Ilyenko, K.E. Makhornin, The bubble frequency in a fluidized bed at elevated pressure, *Powder Technol.* 61 (1990) 251–254.
- [13] R.C. Darton, R.D. LaNauze, J.F. Davidson, D. Harrison, *Trans. Inst. Chem. Eng.* 55 (1977) 274.
- [14] N.S. Grewal, A. Gupta, Total and gas convective heat transfer from a vertical tube to a mixed particle gas–solid fluidized bed, *Powder Technol.* 57 (1989) 27–38.
- [15] D.J. Gunn, N. Hilal, Heat transfer from vertical surfaces to dense gas-fluidized beds, *Int. J. Heat Mass Transfer* 37 (16) (1994) 2465–2473.
- [16] A.C. Hoffmann, J.G. Yates, Experimental observations of fluidized beds at elevated pressures, *Chem. Eng. Commun.* 41 (1986) 133–149.
- [17] A.S. Jensen, Industrial experience in pressurized steam drying of beet pulp, sewage sludge and wood chips, *Drying Technol.* 13 (5–7) (1995) 1377–1393.
- [18] H.S. Mickley, D.F. Fairbanks, Mechanism of heat transfer to fluidized beds, *AIChE J.* 1 (1955) 274–374.
- [19] O. Molerus, W. Mattmann, Heat transfer in gas fluidized beds. Part 2: Dependence of heat transfer on gas velocity, *Chem. Eng. Technol.* 15 (4) (1992) 240–244.
- [20] P.N. Rowe, P.U. Foscolo, A.C. Hoffmann, J.G. Yates, X-ray observation of gas fluidised beds under pressure, in: D. Kunii, R. Toei (Eds.), *Fluidization IV*, Proceedings of the 4th International Fluidization Conference, Sponsored by the Engineering Foundation, Kashikojima, Japan, May 29–June 3, 1983, Engineering Foundation, New York, 1984, pp. 53–60.
- [21] P.S.B. Stewart, J.F. Davidson, *Powder Technol.* 1 (1967) 61.
- [22] A.M. Xavier, D.F. King, J.F. Davidson, D. Harrison, Surface-bed heat transfer in a fluidised bed at high pressure, in: J.R. Grace, J.M. Matsen (Eds.), *Fluidization*, Proceedings of the 1980 International Fluidization Conference, Sponsored by the Engineering Foundation, Henniker, New Hampshire, Aug 3–8, 1980, Plenum Press, New York, 1980, pp. 209–216.